Chemical-Composition-Dependent Metastability of Tetragonal ZrO_2 in Sol−Gel-Derived Films under Different Calcination Conditions

Sue-min Chang† and Ruey-an Doong*

Department of Atomic Science, National Tsing Hua University, 101, Sec. 2, Kuang Fu Road, Hsinchu, 30013, Taiwan

Received June 13, 2005. Revised Manuscript Received July 7, 2005

The chemical compositions at the surface and in the bulk of the sol−gel-derived ZrO_2 films calcined at elevated temperatures in air or in N_2 atmospheres were examined to understand the metastability of the tetragonal phase and the mechanism of its phase transformation. The phase evolution of ZrO_2 in air followed the sequence of amorphous → m-tetragonal → monoclinic over 80−950 °C, while the phase transformation of amorphous → m-tetragonal → monoclinic → m-tetragonal was observed under N_2 atmosphere. The reduction of Zr^{4+} to low-valent states and the generation of oxygen vacancies via dehydroxylation and deoxygenation play the crucial roles in stabilizing m-tetragonal ZrO_2 in the sol−gel-derived films. The O/Zr ratios for stabilizing the m-tetragonal ZrO_2 ranged between 1.98 and 1.63. The m-tetragonal-to-monoclinic phase transformation primarily involves the segregation of lattice defects to grain boundaries and occupation of oxygen vacancies by the diffused O^{2-} ions that were converted from surface hydroxyl groups. In the absence of alternative oxygen donors, including water and oxygen molecules, the stability of m-tetragonal ZrO_2 was maintained at elevated temperatures under N_2 atmosphere. In addition, regeneration of the oxygen vacancies via deoxygenation at high temperature results in the reformation of m-tetragonal ZrO_2. The changes in the chemical compositions and crystallite sizes of the films depict that the m-tetragonal-to-monoclinic phase transformation starts from the core of tetragonal domains, while its retransformation begins from the boundaries of monoclinic grains.

Introduction

Zirconium dioxide (ZrO_2) is a promising material widely used as supports,[1] solid electrolytes,[2] and catalysts[3] because of its special physical and chemical properties such as hardness, ionic conductivity, and surface acidity. These physicochemical properties and technological performance of ZrO_2 have been demonstrated to be greatly controlled by crystalline structures such as crystallite sizes, defects, and crystal phases.[4−6] ZrO_2 mainly contains three polymorphs: monoclinic, tetragonal, and cubic. The monoclinic phase is thermodynamically stable from room temperature to 1200 °C and transforms to the tetragonal form at 1200−2370 °C. The cubic phase appears only at temperatures over 2370 °C.[7] Reversible transformation from a tetragonal to a monoclinic phase in pure ZrO_2 during cooling processes usually causes a volume expansion and catastrophic cracking, thus limiting the application of ZrO_2 to the engineering and electrochemical systems that are operated at high temperatures.[7] This drawback has been overcome by the development of the chemically stabilized tetragonal phase below 1200 °C. However, the stabilized tetragonal ZrO_2 loses its stability gradually and transforms to a monoclinic form at elevated temperatures. Therefore, the investigations on the metastability of tetragonal ZrO_2 attract much attention.

The metastability of tetragonal ZrO_2 in powders has been demonstrated to be related to particle sizes, lattice strain, aggregation tendency, and structure similarity.[8−11] However, such factors have little influence on the metastability of tetragonal ZrO_2 in films because film structures are condensed and the surface areas are fixed before and after phase transformation. The introduction of defects such as allovalent ions into the ZrO_2 lattice has been demonstrated to stabilize the metastable tetragonal phase in powders and films at room temperature.[12] The formation of oxygen vacancies in the metal-doped ZrO_2 is a plausible reason for this stabilization. In addition, the existence of anionic impurities, such as Cl^-, OH^-, SO_4^{2-}, and PO_4^{3-}, in the ZrO_2 lattice has been reported to stabilize m-tetragonal ZrO_2.[13−17] These

* Corresponding author. Tel: +886-3-5726785. Fax: +886-3-5718649. E-mail: radoong@mx.nthu.edu.tw.

† Present address: Institute of Environmental Engineering, National Chiao Tung University, 75, Bo Ai Street, Hsinchu, 300, Taiwan.

(1) Chang, C. C.; Yen, S. K. *Surf. Coat. Technol.* **2004**, *182*, 242.
(2) Politova, T. I.; Irvine, J. T. S. *Solid State Ionics* **2004**, *168*, 153.
(3) De, M.; Kunzru, D. *Catal. Lett.* **2004**, *96*, 33.
(4) Yamaguchi, T. *Catal. Today* **1994**, *20*, 199.
(5) Grau, J. A.; Yori, J. C.; Vera, C. R.; Lovey, F. C.; Condo, A. A.; Parera, J. A. *Appl. Catal. A-Gen.* **2004**, *265*, 141.
(6) Xu, G.; Zhang, Y. W.; Liao, C. S.; Yan, C. H. *Solid State Ionics* **2004**, *166*, 391.
(7) Hannink, R. H. J.; Kelly, P. M.; Muddle, B. C. *J. Am. Ceram. Soc.* **2000**, *83*, 461.
(8) Garvie, R. C. *J. Phys. Chem.* **1965**, *69*, 1238.
(9) Shukla, S.; Seal, S.; Vij, R.; Bandyopadhyay, S.; Rahman, Z. *Nano. Lett.* **2002**, *2*, 989.
(10) Mitsuhashi, T. I. M. T., U. *J. Am. Ceram. Soc.* **1973**, *57*.
(11) Caracoche, M. C.; Rivas, P. C.; Cervera, M. M.; Caruso, R.; Benavidez, E.; de Sanctis, O.; Escobar, M. E. *J. Am. Ceram. Soc.* **2000**, *83*, 377.
(12) Gibson, I. R.; Irvine, J. T. S. *J. Am. Ceram. Soc.* **2001**, *84*, 615.
(13) Cypres, R. W., R.; Raucq, J. *Ber. Dtsch. Keram. Ges.* **1963**, *40*, 527.
(14) Srinivasan, R.; Taulbee, D.; Davis, B. H. *Catal. Lett.* **1991**, *9*, 1.
(15) Srinivasan, R.; Watkins, T. R.; Hubbard, C. R.; Davis, B. H. *Chem. Mater.* **1995**, *7*, 725.
(16) Chokkaram, S.; Srinivasan, R.; Milburn, D. R.; Davis, B. H. *J. Colloid. Interface Sci.* **1994**, *165*, 160.
(17) Spielbauer, D.; Mekhemer, G. A. H.; Riemer, T.; Zaki, M. I.; Knozinger, H. *J. Phys. Chem. B* **1997**, *101*, 4681.

10.1021/cm051264t CCC: $30.25
Published on Web 08/10/2005

results clearly demonstrate that the metastability of tetragonal ZrO_2 is greatly dependent on chemical compositions of ZrO_2. In addition, calcination atmospheres play important roles in the metastability of tetragonal ZrO_2. Calcination under humid or O_2 conditions facilitates the phase transformation from an m-tetragonal to a monoclinic form. It is believed that the phase transformation is mainly related to the infiltration of oxygen vacancies by the adsorbed water or oxygen molecules on oxygen vacant sites at the surface.[18] The chemical compositions changing with calciantion history determine the ionic conductivity, catalytic efficiency, and optical properties of m-tetragonal ZrO_2. Therefore, the characterization of chemical composition of ZrO_2 attracts large devotions not only because of scientific interests but also the impact on applications.

Several instrumental techniques, including electron spin resonance (ESR), nuclear magnetic resonance (NMR), infrared spectroscopy (IR), Rutherford backscattering (RBS), and X-ray photoelectron spectroscopy (XPS), have been used to examine the species in the ZrO_2 to elucidate the mestastability of the tetragonal phase.[10,19] The Zr^{3+} and OH^- were identified in the m-tetragonal phase. In addition, the metastable tetragonal phase shows nonstoichiometric O/Zr values (O/Zr < 2.0), while the phase transformation to monoclinic ZrO_2 usually occurs at an O/Zr ratio close to stoichiometry.[20−22] Guo[23] has used XPS to examine the surface species of ZrO_2 and reports that OH^- ions, in addition to O^{2-} species, are generated after calcination in boiling water. On this basis, a degradation mechanism for m-tetragonal phase was proposed to emphasize that the loss of the stability of the m-tetragonal phase might be due to the occupation of oxygen vacancies by the diffused OH^- ions from the grain surface. However, several studies indicated that removal of OH^- from the ZrO_2 lattice assists the formation of the monoclinic phase.[24] The mechanism for the stabilization of the m-tetragonal phase and the phase transformation to the monoclinic phase are still controversial. Moreover, the mechanism of the degradation of m-tetragonal ZrO_2 under N_2 or vacuum conditions, in which oxygen donors for compensation of lattice oxygen vacancies are absent, is not clear. Therefore, detailed analysis of the chemical compositions throughout the crystallization and phase transformation processes is required.

In this study, the crystalline properties, including phase transformation and crystallite sizes of ZrO_2 films with respect to chemical compositions calcined under air or N_2 atmospheres, were investigated. The O/Zr ratios, species of O, and chemical states of Zr both at the surface and in the bulk of the ZrO_2 films throughout the phase evolution were examined to elucidate the metastability of tetragonal ZrO_2 under these two calcination conditions. Sol−gel method is used for the preparation of ZrO_2 films because it is simple and feasible to control the morphology and thickness of films.

Experimental Section

Preparation of Thin Films. ZrO_2 thin films were prepared using a spin-coated sol−gel method. The sol solution was obtained by fully hydrolyzing $ZrCl_4$ with a stoichiometric quantity of water in 2-propanol (IPA) to yield a Zr:H_2O:IPA molar ratio of 1:4:90. The sol solution was then stored at 25 °C for 24 h to allow equilibrium. An aliquot of the sol solution (20 μL) was spin-coated on a 1.6-cm^2 glass slide, which had been precleaned with $K_2C_2O_7/H_2SO_4$ solution to remove trace amounts of organic contaminants from the surface, at 3000 rpm for 30 s. The temperature and the relative humidity of the ambient atmosphere were controlled at 25 °C and 60%, respectively, during the coating process. This coating cycle was repeated four times to attain a desired film thickness (ca. 35 nm). The as-coated films were then dried at 80 °C for 10 min to evaporate solvents. Calcination was processed in the temperature range between 80 and 950 °C for 12 h in air or in N_2 for crystallization.

Characterization. The morphology and the thickness of the ZrO_2 films were examined by scanning electron microscopy (SEM, Hitachi 4700) operating at an accelerating voltage of 25 kV. All of the SEM samples were platinum-coated. SEM images indicate that the sol−gel-derived ZrO_2 films were smooth and film thicknesses were ca. 35 nm (see Supporting Information, Figure S1). The crystalline properties of the ZrO_2 films were analyzed by an X-ray diffractometer (XRD, Philips X′Pert Pro) using Cu Kα radiation (λ = 1.5406 Å) and operated at an accelerating voltage of 45 kV and an emission current of 40 mA. A grazing angle mode was applied at an incident angle of 1°. Data were acquired over the range of 2θ from 25° to 35° at a sampling width of 0.02° and a scanning speed of 4°/min. The chemical compositions of the ZrO_2 thin films were characterized by an X-ray photoelectron spectrometer (XPS, Physical Electronics, ESCA PHI 1600) using an Al Kα X-ray source (1486.6 eV). After analysis of the chemical composition on the surface, argon etching (operated at 3 kV) was used to remove a 2-nm thickness from the top of the thin films for the analysis of the chemical compositions in the bulk ZrO_2 films. The spherical capacitor analyzer equipped with a multichannel detector and having a takeoff angle of 70° relative to the horizontal plane of the sample was used to collect photoelectrons into the analyzer at a passing energy of 23.5 eV and a collection step of 0.1 eV. All the analytical processes were performed under ultrahigh-vacuum conditions (maintained below 5.0×10^{-9} Torr). The shifts of binding energies of peaks resulted from charging effects were referenced to the Zr $3d_{5/2}$ lined at 182.2 eV.

Data Management. Volume Percentage of Phases. The volume fraction of the tetragonal (χ_t) and monoclinic (χ_m) phases were estimated from the integrated peak intensity of the $(101)_t$ plane of the tetragonal phase (I_t) and the $(111)_m$ and $(\bar{1}11)_m$ planes of the monoclinic phase (I_m) using the following equations:[25]

$$\chi_t = \frac{I_t(101)}{I_t(101) + I_m(111) + I_m(\bar{1}11)} \quad (1)$$

$$\chi_m = 1 - \chi_t \quad (2)$$

Crystallite Sizes. The average crystallite sizes of the tetragonal and monoclinic phases were calculated from the broadening of diffraction lines of the tetragonal (101) and monoclinic (111)

(18) Srinivasan, R.; Hubbard, C. R.; Cavin, O. B.; Davis, B. H. *Chem. Mater.* **1993**, *5*, 27.
(19) Wang, H. C.; Lin, K. L. *J. Mater. Sci.* **1991**, *26*, 2501.
(20) Venkataraj, S.; Kappertz, O.; Weis, H.; Drese, R.; Jayavel, R.; Wuttig, M. *J. Appl. Phys.* **2002**, *92*, 3599.
(21) Koski, K.; Holsa, J.; Juliet, P. *Surf. Coat. Technol.* **1999**, *121*, 303.
(22) Marinsek, M.; Macek, J.; Meden, T. *J. Sol−Gel Sci. Technol.* **2002**, *23*, 119.
(23) Guo, X. *J. Phys. Chem. Solids* **1999**, *60*, 539.
(24) Caracoche, M. C.; Rivas, P. C.; Cervera, M. M.; Caruso, R.; Benavidez, E.; de Sanctis, O.; Mintzer, S. R. *J. Mater. Res.* **2003**, *18*, 208.
(25) Stefanic, G.; Music, S. *Croat. Chem. Acta* **2002**, *75*, 727.

Table 1. Average Crystallite Sizes of the m-Tetragonal and Monoclinic Phases Calcined at Various Temperatures

	in air		in N_2			in air		in N_2	
temp (°C)	D_{101} (nm)[a]	D_{111} (nm)[b]	D_{101} (nm)[a]	D_{111} (nm)[b]	temp (°C)	D_{101} (nm)[a]	D_{111} (nm)[b]	D_{101} (nm)[a]	D_{111} (nm)[b]
400	15.4	–	NA[d]	NA	650	12.0	16.5	15.4	–
450	15.4	–	18.5	–	700	–[c]	18.0	15.8	16.2
500	16.3	–	NA	NA	750	–	18.4	5.0	16.9
550	14.8	10.9	17.5	–	850	–	15.8	8.1	15.6
600	14.3	15.3	15.7	–	950	–	15.6	9.3	15.3

[a] Crystallite size of $(101)_t$ profile. [b] Crystallite size of $(111)_m$ profile. [c] Not detected. [d] NA means not available.

profiles using the Scherrer equation:[26]

$$D_{hkl} = \frac{0.9\lambda}{\beta_{hkl}\cos\theta} \tag{3}$$

where D_{hkl} is the average crystallite size of the (*hkl*) profile, λ is the wavelength of the incident X-rays (Cu Kα = 1.5406 Å), β_{hkl} is the full width at half-maximum (fwhm) of the (*hkl*) line, and θ is the Bragg angle.

Curve Fitting of the XPS Spectra. After performing a Shirley-type background subtraction, the original spectra were fitted using a nonlinear least-squares fitting program and Gaussian−Lorentzian peak shapes were adapted for all the peaks. The parameters used for the curve fitting of the Zr 3d and O 1s spectra, including the binding energies, the doublet separation, and the full-width at half-maximum (fwhm) of Zr $3d_{5/2}$ are summarized in Table 1S (See Supporting Information, Table 1S). Morant et al.[27] depicted that the oxidation states of Zr were separated by an energy shift of 1.06 eV in the ZrO_2 matrix. In the present study, the binding energy of Zr^{4+} $3d_{5/2}$ at 182.2 eV was taken, and the low oxidation states of Zr (Zr^{3+}, Zr^{2+}, and Zr^{+}) were downshifted by 1.06 eV per oxidation state with respect to Zr^{4+}. The fwhm of Zr $3d_{5/2}$ was set to 1.7 eV with a doublet separation of 2.37 or 2.39 eV to Zr $3d_{3/2}$. The binding energies of O 1s for the Zr−O and Zr−OH species were set at 529.9 and 531.7 eV, respectively, with doublet separations of 1.6−1.9 and 1.9−2.3 eV, respectively. The atomic ratios were calculated from the integrated peak areas normalized to sensitivity factors of 2.576 and 0.711 for Zr and O, respectively.

Results

Crystalline Properties of ZrO_2 Films Calcined in Different Atmospheres. Figure 1 presents the XRD patterns of ZrO_2 films calcined in different atmospheres. When the films were calcined in air, the sol−gel-derived ZrO_2 thin film was amorphous initially and began to crystallize into an m-tetragonal phase as the temperature increased to 400 °C. The m-tetragonal phase was stable in the ZrO_2 thin film at 400−500 °C, and the phase transformation from the m-tetragonal to a monoclinic phase occurred at 550 °C with an m-tetragonal-to-monoclinic volume ratio of 35:65 (see Supporting Information, Figure S2). The fraction of monoclinic ZrO_2 increased upon increasing calcination temperature, and the progressive transformation was complete at 700 °C.

Similar to the results obtained in air, the sol−gel-derived ZrO_2 film calcined in N_2 initially crystallized into the m-tetragonal phase and then a phase transformation occurred to a monoclinic form. The m-tetragonal-to-monoclinic phase transformation occurred, however, at 700 °C, which is higher than that observed in air. Moreover, the maximal conversion of the m-tetragonal phase to the monoclinic phase was only 96% at 750 °C, and 4% m-tetragonal phase still remained. As the calcination temperature rose to 850 °C, the monoclinic phase retransformed to the tetragonal phase. The volume fraction of the tetragonal phase increased to 15% upon increasing the temperature to 950 °C. However, the monoclinic-to-tetragonal phase transformation was not observed for the ZrO_2 thin films calcined in air within the experimental temperature range in this study.

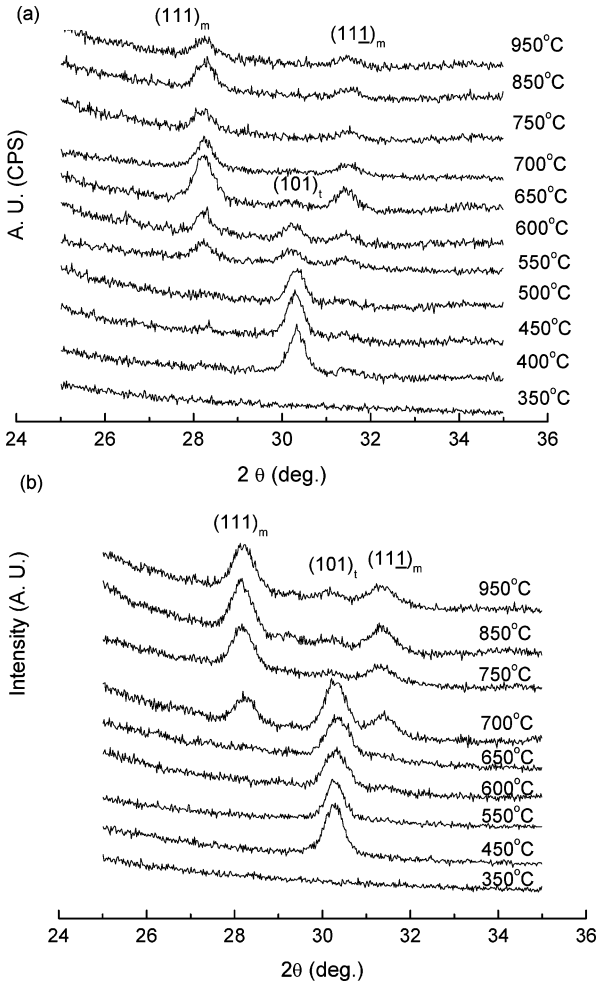

Figure 1. XRD patterns of the ZrO_2 thin films calcined (a) in air and (b) in N_2 for 12 h.

Table 1 shows the average crystallite sizes measured at the elevated temperatures in different atmospheres. Under the atmosphere of air, the crystallite size of m-tetragonal ZrO_2 was 15.4 nm at 400 °C and slightly increased to 16.3 nm as the temperature increased to 500 °C. The crystallite size of m-tetragonal ZrO_2 diminished to 12.0 nm at 650 °C, the temperature at which the m-tetragonal-to-monoclinic phase transformation occurred. The monoclinic phase formed initially at 550 °C with a crystallite size of 10.9 nm, and the crystallite size increased to 16.5 nm when the m-tetragonal-to-monoclinic phase transformation completed at 750 °C. The crystallite sizes then decreased to 15.6 nm as the temperature increased to 950 °C.

(26) Stefanic, G.; Stefanic, I. I.; Music, S. *Mater. Chem. Phys.* **2000**, *65*, 197.
(27) Morant, C. S. J. M. G., L.; Soriano, L.; Rueda, F. *Surf. Sci.* **1989**, *218*, 331.

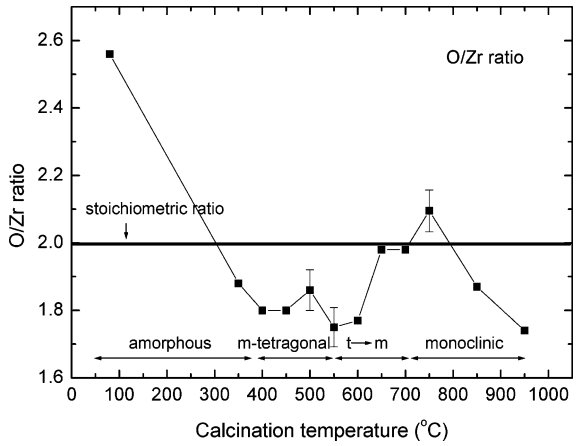

Figure 2. The evolution of lattice O/Zr ratios when the ZrO_2 thin films calcined in air.

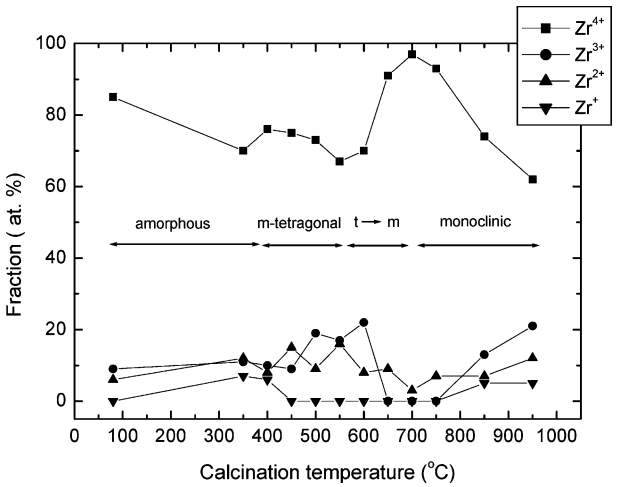

Figure 3. The fractions of Zr species in the bulk ZrO_2 films calcined in air as a function of the calcination temperature.

Under the atmosphere of N_2, the crystallite size of the $(101)_t$ profile decreased from 18.5 to 15.4 nm as the temperature increased from 450 to 650 °C. During the m-tetragonal-to-monoclinic phase transformation, the crystallite sizes of the $(101)_t$ and the $(111)_m$ profiles were 15.8 and 16.2 nm, respectively, which were rather close. However, the crystallite sizes of the $(101)_t$ and $(111)_m$ profile were 5.0 and 16.9 nm, respectively, at the maximal phase transformation temperature of 750 °C. As the monoclinic phase transformed to the tetragonal phase at 850−950 °C, the crystallite size of the $(111)_m$ profile decreased to 15.3−15.6 nm. Meanwhile, the crystallite size of the $(101)_t$ profile slightly increased from 8.1 to 9.3 nm over this temperature range.

Chemical Compositions in Bulk ZrO_2 Films Calcined in Air. To elucidate the relationship between the chemical compositions and the crystalline properties, the lattice O/Zr ratios and the chemical states of the O and Zr ions in the bulk were examined after removing a 2-nm-thick layer from the top of the thin films. Figure 2 shows the lattice O/Zr ratios in the bulk ZrO_2 films as a function of temperature. The O/Zr ratio of the as-dried ZrO_2 was 2.56, which indicates that many hydroxyl groups generated during the hydrolysis remained in the sol−gel-derived ZrO_2 structure before calcination. These hydroxyl groups were removed from the thin films upon thermal treatment, resulting in the decrease in O/Zr ratios. The O/Zr ratios ranging between 1.77 and 1.88 were observed at 400−600 °C, the temperature range in which the m-tetragonal phase was stable. These values are below the stoichiometric value (O/Zr = 2), which suggest the existence of oxygen deficiencies. As the temperature increased to 650−750 °C, the m-tetragonal phase was completely transformed into the monoclinic phase and the O/Zr ratios increased to near stoichiometric values. The O/Zr ratios fell again, however, to nonstoichiometric values (O/Zr < 2) at temperatures above 750 °C.

The XPS spectra of O 1s in the ZrO_2 lattice can be deconvoluted into Zr−O and Zr−OH peaks by curve fitting (see Supporting Information, Figure S3). The atomic ratios estimated from their peak areas indicate that the Zr−OH species were 18% to the total oxygen content in the as-dried ZrO_2 film. After calcination, the fraction of Zr−OH decreased to a relatively stable value of 10−12% over the temperature range of 350−950 °C because of the removal of the lattice hydroxyl groups. The curve fittings of the Zr 3d spectra clearly indicate that, besides the dominant Zr^{4+} species, Zr^{3+}, Zr^{2+}, and Zr^{+} were present in small amounts after calcination. This phenomenon indicates that some Zr^{4+} ions were reduced to low-valent states in the nonstoichiometric ZrO_2 films as a result of charge compensation.

Figure 3 shows the fractions of the Zr species as a function of the calcination temperature. The Zr^{4+} ions constituted 85% of the total Zr in the as-dried thin film and decreased to 67−76% at 350−600 °C. An increased fraction of Zr^{4+} ions (91−97%) appeared as the temperature increased to 650−750 °C, at which the phase transformed to the monoclinic phase. The Zr^{4+} fractions decreased again to 62% at 750−950 °C. In addition, the fractions of the Zr^{3+}, Zr^{2+}, and Zr^{+} ions varied as a result of the Zr^{4+} fraction changing at the different temperatures. The Zr^{3+} atoms, which were the second-most dominant species, accounted for 9−22% of the total Zr at the experimental temperature ranges. The Zr^{2+} and Zr^{+} ions contained 3−16% and 5−17% to total Zr species, respectively.

Chemical Compositions at the Surface of ZrO_2 Films Calcined in Air. The changes in the lattice O/Zr ratios and the fractions of Zr species indicate that thermal treatment not only drives oxygen out of the thin films but also causes an intake of oxygen from the air into the thin films. To clarify the process of oxygen recovery, the Zr and O species and their atomic ratios at the surface were investigated. The XPS spectra of Zr 3d and O 1s characterized at the surface of ZrO_2 films reveals that the surface contained only Zr^{4+} species. In addition, substantial numbers of hydroxyl groups were bonded at the surface (see Supporting Information, Figure S4). Figure 4 presents the surface O/Zr, Zr−O/Zr, and Zr−OH/Zr ratios at different calcination temperatures in air. In agreement with the lattice O/Zr ratios, the surface O/Zr ratios decreased from 2.90 to 2.27 as the temperature increased from 80 to 500 °C. A remarkable increase in the surface O/Zr ratio to 2.59−2.66 was observed, however, in the temperature range 550−600 °C, at which temperatures the m-tetragonal-to-monoclinic phase transformation occurred. Subsequently, the surface O/Zr ratio dropped suddenly to 2.27 at 650 °C and increased again at 700−950 °C.

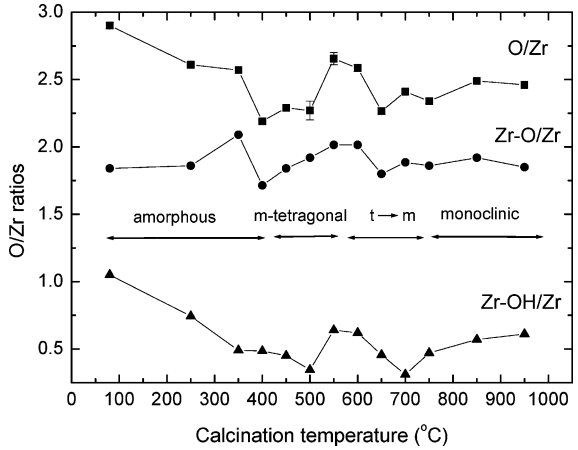

Figure 4. Surface O/Zr, Zr−O/Zr, and Zr−OH/Zr ratios plotted as a function of the temperature of ZrO_2 film calcination in air.

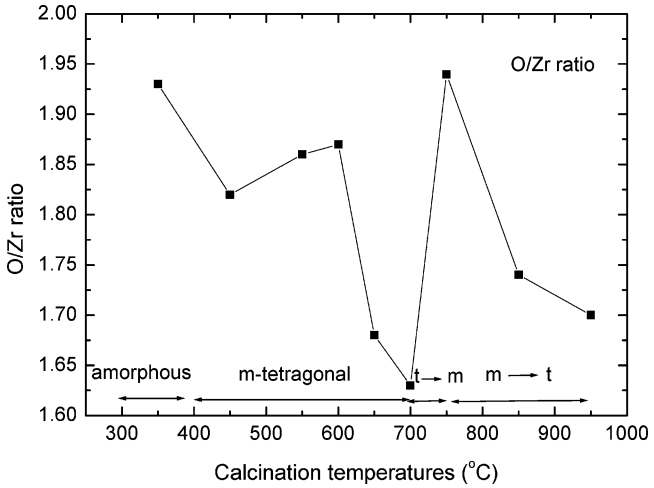

Figure 5. The O/Zr ratio in bulk ZrO_2 films plotted as a function of the calcination temperature in N_2.

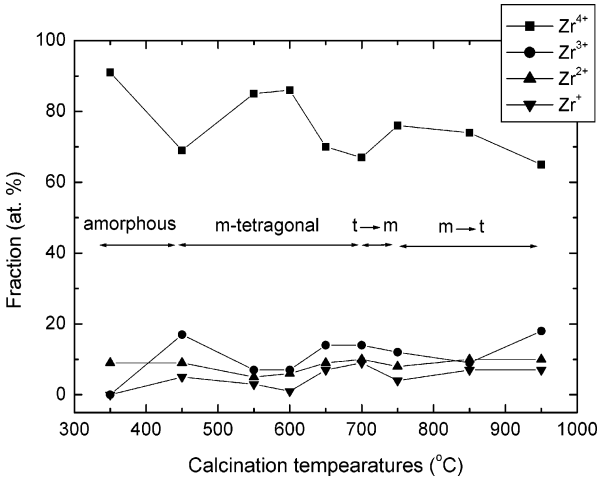

Figure 6. Fractions of Zr species in bulk ZrO_2 films plotted as a function of the calcination temperature in N_2.

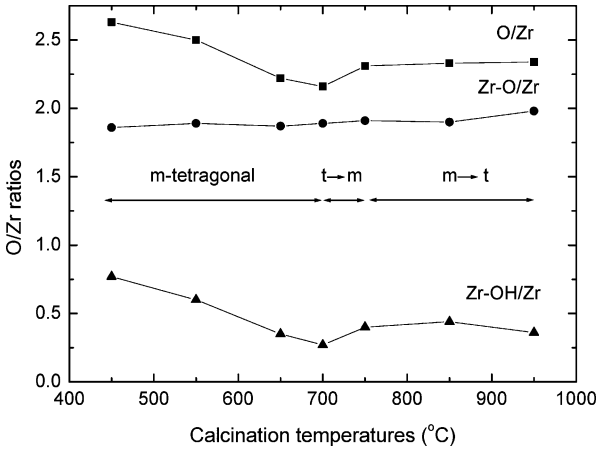

Figure 7. The O/Zr, Zr−O/Zr, and Zr−OH/Zr ratios as a function of calcination temperatures in N_2.

In addition, the changes in the Zr−OH/Zr and Zr−O/Zr ratios as a function of temperature were investigated. The Zr−OH/Zr ratios decreased from 1.05 to 0.35 as the temperature increased from 80 to 500 °C, indicating that dehydroxylation occurred upon thermal treatment. The Zr−OH/Zr ratio then increased to 0.62−0.64 at 550−600 °C before falling to 0.31 at 700 °C. Again, the Zr−OH/Zr ratio gradually increased to 0.61 over the range between 750 and 950 °C. In contrast to the surface Zr−OH/Zr ratios, the surface Zr−O/Zr ratios increased initially from 1.84 to 2.09 upon increasing the temperature from 80 to 350 °C, which implies that some Zr−OH were converted to Zr−O groups during the dehydroxylation process. The Zr−O/Zr ratio fell to a substoichiometric value (1.72) at 400 °C, the temperature at which the thin film crystallized into the m-tetragonal phase. It is noted that the Zr−O/Zr ratio increased to the stoichiometric value (2.02) at 550−600 °C during the phase transformation and then fell to 1.80−1.92 at 650−950 °C.

Chemical Compositions in Bulk ZrO_2 Films Calcined in N_2. Figure 5 presents the lattice O/Zr ratios of ZrO_2 thin films calcined in N_2 as a function of the calcination temperature. The lattice O/Zr ratios in the bulk ZrO_2 films were all below the stoichiometric value (O/Zr = 2). An O/Zr ratio of 1.93 was observed in amorphous ZrO_2 calcined at 350 °C, and then it decreased to 1.82−1.87 as the temperature increased to 400−600 °C. A significant decrease in the O/Zr ratio to 1.63 occurred over the temperature range 600−700 °C and then a remarkable increase to 1.94 appeared at 750 °C, the temperature at which the maximal m-tetragonal-to-monoclinic transformation occurred. Further increases in the calcination temperature to 950 °C caused the O/Zr ratio to decline to 1.70. Figure 6 displays the fractions of the four Zr species—Zr^{4+}, Zr^{3+}, Zr^{2+}, and Zr^{+}—in the ZrO_2 thin films calcined in N_2 at various temperatures. The fraction of Zr^{4+} decreased initially from 91 to 69% as the crystalline structure changed from an amorphous to the m-tetragonal phase at 350−450 °C. Before the next decrease in the fraction of Zr^{4+} to 67% at 650−700 °C, the content of Zr^{4+} increased to 86% at 450−600 °C. The Zr^{4+} content again increased to 76% at 750 °C and gradually fell to 65% as the temperature was increased to 950 °C. The fractions of the Zr^{3+}, Zr^{2+}, and Zr^{+} ions at elevated temperatures were in the range of 7−18%, 5−10%, and 1−9%, respectively, which exhibit an opposite trend to that of Zr^{4+} ions.

Chemical Compositions at the Surface of ZrO_2 Films Calcined in N_2. Figure 7 plots the O/Zr, Zr−O/Zr, and Zr−OH/Zr ratios at the surface of the ZrO_2 thin films as a function of the calcination temperature under N_2 atmosphere. The Zr−OH/Zr ratio fell from 0.77 at 450 °C to its minimal value of 0.27 at 700 °C and slightly increased to 0.36 at

950 °C. In contrast to the change in the Zr−OH/Zr ratio, the Zr−O/Zr ratio remained within 1.86−1.98 in the temperature range of 450−950 °C. The O/Zr ratio was primarily dominated by the Zr−OH/Zr ratio and exhibited a minimal value of 2.16 at 700 °C.

Discussion

Calcination in Air. The m-tetragonal phase is stable at 400−650 °C in pure sol−gel-derived ZrO_2 thin films when calcined in air. Calcination in N_2 extends the stability of the m-tetragonal phase up to 750 °C. The changes in the O/Zr ratios and the chemical states of Zr clearly depict the formation and annihilation of oxygen vacancies and their roles in the stabilization of the tetragonal phase in the sol−gel-derived ZrO_2 films. Hydrolysis during the sol−gel process usually introduces hydroxyl groups into the amorphous ZrO_2 structure. The decrease in the content of lattice Zr−OH indicates that the hydroxyl groups are driven out from the ZrO_2 thin films in the form of water molecules upon thermal treatment. Meanwhile, the elements in the ZrO_2 sample rearrange into a crystalline form. The dehydroxylation reduces Zr^{4+} to low-valent states and also results in oxygen vacancies for charge compensation according to following equations:

$$Zr^{4+}\cdots{}^{-}OH + HO^{-}\cdots Zr^{4+} \rightarrow Zr^{3+}\cdots V_{oxygen} + Zr^{4+}\cdots O^{-} + H_2O \quad (4)$$

$$Zr^{3+}\cdots{}^{-}OH + HO^{-}\cdots Zr^{4+} \rightarrow Zr^{2+}\cdots V_{oxygen} + Zr^{4+}\cdots O^{-} + H_2O \quad (5)$$

$$Zr^{2+}\cdots{}^{-}OH + HO^{-}\cdots Zr^{4+} \rightarrow Zr^{+}\cdots V_{oxygen} + Zr^{4+}\cdots O^{-} + H_2O \quad (6)$$

where V_{oxygen} means an oxygen vacancy. The oxygen vacancies are considered to be responsible for the formation of m-tetragonal phase instead of forming the thermodynamically stably monoclinic phase upon crystallization. Usually, oxygen vacancies are introduced by incorporation of allovalent ions, including Y^{3+}, Mg^{2+}, and Ca^{2+}, into the ZrO_2 lattice.[28,29] The autoreduced Zr species in the sol−gel-derived ZrO_2 films explain why the tetragonal phase can be stabilized in the pure ZrO_2.

The phase transformation from m-tetragonal to monoclinic phase began at 550 °C and completed at 700 °C. Meanwhile, the lattice O/Zr ratios changed from substoichiometric (<2) to almost stoichiometric (≅ 2) values, which indicates that the monoclinic phase tends to be stabilized when ZrO_2 approaches stoichiometry. The increase in the lattice O/Zr ratios reveals that an intake of oxygen from air into the thin film induces the phase transformation from m-tetragonal to monoclinic phase. Srinivasan et al.[18] have reported that the phase transformation from m-tetragonal to monoclinic form occurs rapidly in an oxygen-containing atmosphere than in helium. On this basis, the phase transformation as a result of a surface phenomenon has been proposed. In addition, the m-tetragonal-to-monoclinic transformation involving the existence of water vapor and oxygen molecules has been proposed by several studies.[30−32] In this study, the increasing Zr−OH/Zr and Zr−O/Zr ratios at the surface suggest that the intake of oxygen begins with the adsorption of water and oxygen from air onto the surface. The adsorbed water and oxygen molecules are then dissociated into hydroxyl ions and oxygen atoms to fill the oxygen vacancies at the surface. Similar results are also reported in Guo's studies, which investigated the degradation mechanism of tetragonal ZrO_2 in Y-doped matrix.[33] In this study, the subsequent decreases in the surface Zr−OH/Zr and Zr−O/Zr ratios at 650−700 °C reveal that the surface-bound oxygen species diffuse into the thin films. Several studies have proposed that the surface OH groups diffuse into inner ZrO_2 and consequently occupy oxygen vacancies to promote m-tetragonal → monoclinic phase transformation.[23,33] In this study, the content of lattice OH groups did not increase before and after the phase transformation. This finding depicts that the surface-bound oxygen species mainly convert into oxygen ions (O^{2-}) that can penetrate into the ZrO_2 thin films to induce the phase transformation. Meanwhile, the low-valent Zr species in the lattice again oxidized to Zr^{4+} by the diffused oxygen ions.

After the phase transformation to the monoclinic form was complete, the lattice O/Zr ratios decreased as the temperature rose above 750 °C. Accordingly, some oxygen atoms were eliminated from the thin film at elevated temperatures. This thermally induced deoxygenation involves the donation of two electrons and the reduction of Zr^{4+} to low-valent states according to the following equations:

$$Zr^{4+}\cdots{}^{-}O^{-}\cdots Zr^{4+} + Zr^{4+}\cdots{}^{-}O^{-}\cdots Zr^{4+} \rightarrow O_2 + Zr^{3+}\cdots V_{oxygen}\cdots Zr^{3+} + Zr^{3+}\cdots V_{oxygen}\cdots Zr^{3+} \quad (7)$$

$$Zr^{3+}\cdots{}^{-}O^{-}\cdots Zr^{3+} + Zr^{3+}\cdots{}^{-}O^{-}\cdots Zr^{3+} \rightarrow O_2 + Zr^{2+}\cdots V_{oxygen}\cdots Zr^{2+} + Zr^{2+}\cdots V_{oxygen}\cdots Zr^{2+} \quad (8)$$

$$Zr^{2+}\cdots{}^{-}O^{-}\cdots Zr^{2+} + Zr^{2+}\cdots{}^{-}O^{-}\cdots Zr^{2+} \rightarrow O_2 + Zr^{+}\cdots V_{oxygen}\cdots Zr^{+} + Zr^{+}\cdots V_{oxygen}\cdots Zr^{+} \quad (9)$$

Although oxygen vacancies and reduced Zr species were regenerated within the thin films, the transformation from the m-tetragonal to the monoclinic phase did not occur. To maintain the stability of the monoclinic phase under the nonstoichiometric conditions, the reduced Zr species and oxygen vacancies might segregate from the monoclinic ZrO_2 domain and consequently resulted in the decrease in the crystallite size at 850−950 °C. Such segregation has been observed for doped ZrO_2 at high temperatures.[34,35] In addition, the deoxygenation increases numbers of oxygen vacancies at the film surface and provides extra binding sites for hydroxyl groups, which can be evidenced by the increased surface Zr−OH/Zr ratio at temperatures above 750 °C.

(28) Zhang, Y. W.; Yang, Y.; Tian, S. J.; Liao, C. S.; Yan, C. H. *J. Mater. Chem.* **2002**, *12*, 219.
(29) Dell'Agli, G.; Mascolo, G. *J. Eur. Ceram. Soc.* **2004**, *24*, 915.
(30) Xie, S. B.; Iglesia, E.; Bell, A. T. *Chem. Mater.* **2000**, *12*, 2442.
(31) Li, M. J.; Feng, Z. C.; Zhang, J.; Ying, P. L.; Xin, Q.; Li, C. *Chin. J. Catal.* **2003**, *24*, 861.
(32) Collins, D. E.; Bowman, K. J. *J. Mater. Res.* **1998**, *13*, 1230.
(33) Guo, X. *Solid State Ionics* **1998**, *112*, 113.
(34) Ram, S. *J. Mater. Sci.* **2003**, *38*, 643.
(35) Chang, S. M.; Doong, R. A. *J. Phys. Chem. B* **2004**, *108*, 18098.

Scheme 1. Schematic Diagram of the Proposed Mechanism for the m-Tetragonal-to-Monoclinic Phase Transformation and Its Retransformation in N_2[a]

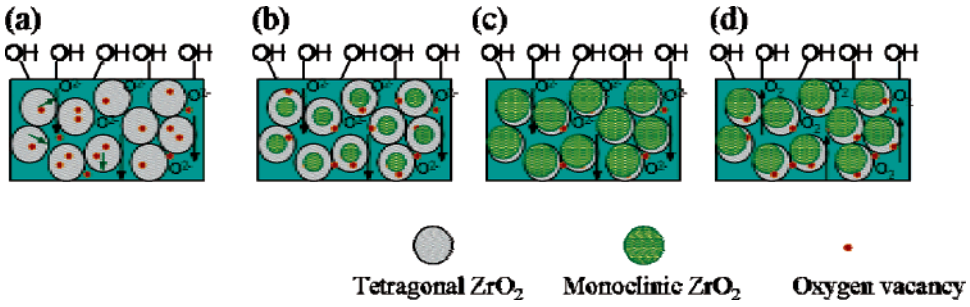

[a] (a) Diffusion of O^{2-} from film surface into interior ZrO_2 and segregation of oxygen vacancies from m-tetragonal ZrO_2 domain to the grain boundaries, (b) the occurrence of m-tetragonal-to-monoclinic phase transformation from cores of m-tetragonal domains, (c) growth of monoclinic domains, and (d) regeneration of oxygen vacancies via deoxygenation and the phase retransformation starting from the boundaries of monoclinic domains.

Normally, the monoclinic-to-tetragonal phase transformation occurs at temperatures above 1200 °C and a displaced tetragonal-to-monoclinic phase transformation is undergone at 950 °C during cooling.[7] In this study, the increase in the Zr−OH/Zr ratios at the surface of the monoclinic films depicts that the surface hydroxyl groups could compensate the oxygen vacancies and might be responsible for this reversible phase transformation.

Calcination in N_2. Calcination in N_2 retards m-tetragonal-to-monoclinic phase transformation from 550 to 700 °C because of the maintenance of oxygen vacancies in the absence of oxygen donors such as water and oxygen. The mechanism of the crystallization of the sol−gel-derived ZrO_2 thin films calcined in N_2 is similar to the mechanism that occurs in air. The dehydroxylation generates oxygen vacancies to stabilize the m-tetragonal phase at room temperature. Although alternative oxygen donors such as water and oxygen molecules are absent in N_2, the O/Zr ratio in bulk ZrO_2 increased over the temperature range 450−600 °C. The decrease in the number of surface Zr−OH species indicates that the surface hydroxyl groups of sol−gel-derived ZrO_2 are consumed to compensate the lattice oxygen vacancies. The annihilation of oxygen vacancies could promote the formation of the monoclinic phase.

It has been proposed that the m-tetragonal-to-monoclinic phase transformation starts from the surface of the m-tetragonal grain boundary.[9,33] The mechanism for this phase transformation involves the penetration of OH^- through the grain boundary into the inner part. By annihilation of oxygen vacancies from the occupied OH^- in the boundary, the m-tetragonal ZrO_2 transformed to monoclinic form in the surface layer of m-tetragonal grains. However, results shown in this study demonstrate that the phase transformation from m-tetragonal to monoclinic ones involves the segregation of oxygen vacancies and possibly begins from the core of m-tetragonal domains. Scheme 1 illustrates the proposed mechanism for m-tetragonal-to-monoclinic phase transformation and its retransformation. As the temperature further increases to 600−700 °C, the decreasing O/Zr ratio in the bulk ZrO_2 indicates that the oxygen vacancies are reformed via eqs 7−9. Although the surface hydroxyl groups are still converted to O^{2-} to fill the oxygen vacancies under this circumstance, the diffusion rate of O^{2-} is lower than the rate at which the oxygen vacancies are generated. The oxygen-deficient conditions result in the reduction of Zr^{4+} to low-valent species in the bulk ZrO_2. In addition, the crystallite sizes of the m-tetragonal ZrO_2 diminished upon increasing temperatures. These findings reveal that the oxygen vacancies and the reduced Zr species segregate from the m-tetragonal domains to their boundary at elevated temperatures. This segregation decreases the number of oxygen vacancies in the m-tetragonal domains and induces the transformation of m-tetragonal domains into the monoclinic form. Because the crystallite sizes of the m-tetragonal (15.8 nm) and monoclinic (16.2 nm) ZrO_2 samples are very similar in this study, it is believed that the monoclinic domains are converted from the m-tetragonal domains. As the lattice O/Zr ratio increased to 1.94, i.e., close to stoichiometry, the m-tetragonal phase almost transformed into the monoclinic form. It is worth noting that the transformation from the monoclinic phase back to the m-tetragonal phase occurred at a temperature above 750 °C. Meanwhile, both the O/Zr ratio and the Zr^{4+} content in the bulk ZrO_2 decreased upon increasing temperatures, which indicates that further deoxygenation at high-temperature results in the formation of oxygen vacancies and, thus, triggers the monoclinic-to-m-tetragonal conversion. Both the fraction and crystallite sizes of m-tetragonal phase increased with the increasing temperatures. This finding depicts that the stabilization of the tetragonal phase starts at the boundary of monoclinic grains and progresses into their interior. Similar behavior is also observed in Y-doped ZrO_2 calcined in N_2 at high temperatures, in which the m-tetragonal phase is stabilized by incorporation of nitrogen ions at the surface of grains.[36]

Guo[33] has proposed that critical maximum and minimum vacancy concentrations should exist for the formation of the stable m-tetragonal phase. In this study, the minimum O/Zr ratio required to stabilize the m-tetragonal phase was 1.63 at 700 °C in N_2, while the maximum O/Zr ratio of 1.98 was obtained at 650 °C in air. When the O/Zr ratio was higher than this maximum value (1.98), the m-tetragonal phase transformed completely into the monoclinic phase. On the other hand, segregation of low-valent Zr species to form suboxides (Zr_2O_3) would occur when the O/Zr ratio is below the minimum value (1.63).

(36) Chung, T. J.; Song, H. S.; Kim, G. H.; Kim, D. Y. *J. Am. Ceram. Soc.* **1997**, *80*, 2607.

Conclusions

Results obtained in this study clearly demonstrate that the chemical compositions of ZrO_2, which vary with respect to the calcination temperatures and atmospheres, govern the evolution of crystalline phases. Dehydroxylation and deoxygenation processes in the sol−gel-derived ZrO_2 films reduce Zr^{4+} atoms to low-valent states and generate oxygen vacancies to stabilize the m-tetragonal phase. The calcination atmosphere determines the fate of oxygen vacancies, the metastability of m-tetragonal ZrO_2, and the mechanism of phase transformation. Calcination in air increases the amount of surface hydroxyl groups and reduces the number of oxygen vacancies through the diffused oxygen ions from the surface to facilitate the phase transformation. The monoclinic phase is stable when the composition is close to the stoichiometric value. On the other hand, calcination in N_2 sustains the oxygen vacancies, resulting in the increase in the stability of the m-tetragonal phase. The phase transformation predominantly involves segregation of the oxygen vacancies and the intake of surface hydroxyl groups to fill these vacancies. In addition, deoxygenation increases the number of oxygen vacancies at high temperature under N_2 atmosphere and triggers the phase transformation from the monoclinic phase back to the m-tetragonal phase. The minimal and maximal O/Zr ratios for maintaining the stability of the m-tetragonal phase are 1.63 and 1.98, respectively. In summary, results of this study not only demonstrate directly the crystalline characteristics of the sol−gel-derived ZrO_2 with respect to the chemical compositions but also provide detailed information regarding the defects that occur, which may lead to a better understanding of the catalytic and conductive properties of structural ZrO_2.

Acknowledgment. The authors thank the National Science Council, Taiwan, R.O.C., for the financial support under grant No. NSC93-2113-M-007-039.

Supporting Information Available: SEM images of the sol−gel-derived ZrO_2 films, the volume fraction of m-tetragonal and monoclinic ZrO_2 in the thin films calcined at elevated temperatures in air or in N_2, Zr 3d and O1s spectra acquired from the surface of or inside the ZrO_2 films, and parameters for curve fitting the Zr 3d and O 1s photoelectron spectra. This material is available free of charge via the Internet at http://pubs.acs.org.

CM051264T